

INVESTIGATION INTO THE ROLE OF SINGLET OXYGEN IN POSITIVE CORONA IN AIR

A.G. Swanson* and I.R. Jandrell*†

* School of Electrical and Information Engineering, Faculty of Engineering and the Built Environment, Private Bag 3, Wits 2050, South Africa E-mail: andrewgswanson@gmail.com

† E-mail: ian.jandrell@wits.ac.za

Abstract: Corona is the partial breakdown of air in a divergent electric field and is particularly evident around high voltage equipment. Air comprises of nitrogen and oxygen and the corona process involves many complex phenomena including ionisation, attachment and excitation and the interaction of the ions and excited molecules generated by these phenomena. A particular state of excited molecular oxygen, singlet oxygen, has the characteristic that it remains excited for a relatively long period of time. Singlet oxygen plays a role in the detachment of electrons from the negative oxygen ions and its role in corona discharges has been accounted for through theory and models, but due to the difficulties of measurement of the singlet oxygen, the influence it does have on corona discharges is not entirely clear. On this basis the gas processes associated with the corona discharge in air have been explored, where a Boltzmann equation solver, the electron energy distribution function, transport coefficient and Townsend coefficients are used to understand the phenomena and provide input to a gas discharge model, where the gases are representing as species in a drift-diffusion model. The model indicates the presence of negative ions and singlet oxygen, but clearly illustrates how the space charge plays the critical role in positive corona due to the collapse of the electric field. An experiment that involved altering the environment with air-flow produced an unexpected result in the positive onset streamers where the repetition rate changed considerably, initially it was thought that this was due to the removal of singlet oxygen. In an effort to determine if there was a relationship between repetition rate and singlet oxygen, experiments detecting the emission from singlet oxygen and exciting oxygen through a laser were undertaken. There was no evidence to suggest that the repetition rate of the positive onset streamers could be related to singlet oxygen. There were no emissions detected from various configurations, whilst visible corona was clearly seen. The experiment where laser induced excitation showed no change in repetition rate. It could be inferred that a relationship between repetition rate and that the detachment due to negative ions and singlet oxygen is not a dominant process in the corona discharge.

Key words: Corona, Positive onset streamers, Space charge, Singlet oxygen

1. INTRODUCTION

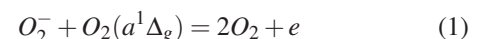
Corona in air is the partial breakdown of the gas in a sufficiently high electric field. For high voltage engineering it is responsible for audio and radio interference and is a sign of poorly designed or degraded hardware or materials.

Air is predominantly made up of nitrogen and oxygen and corona occurring in air involves many complex phenomena including the production of space charge and excited molecular states of its constituents. Oxygen itself is an electronegative gas and has the ability to attach electrons. In the discharge process these phenomena combine to influence the electric field and the production of secondary electrons give corona its distinctive modes [1].

Positive corona involves electrons that are produced by natural means and move towards the high voltage electrode. This causes a number of reactions including ionisation, attachment and excitation and a subsequent collapse of the electric field. The process can only begin again when the space charge dissipates [1, 2]. The main difference with negative corona is that in negative corona the electrons are emitted upon positive

ion bombardment with the electrode producing a supply of seed electrons are responsible for the repetitive nature of Trichel pulses, whereas positive corona has no such measurable mechanism to produce such seed electrons [1, 2].

Singlet oxygen, $O_2(a^1\Delta_g)$, is the lowest electronic excited state of oxygen and it has the characteristic that it remains in the excited state for a relatively long amount of time. Lowke proposed in his work that the singlet oxygen has a dominant role in the pre-breakdown corona and streamer process because of its ability to detach electrons from negative ions as given by the reaction [3, 4]:



An initial experiment was performed in [5] where the application of airflow to a point plane gap initially intended to alter the space charge produced an interested phenomena, where the low speed airflow significantly changed the repetition rate of positive onset streamers. This did not seem consistent with theory and considering the reaction in Equation (1), it was hypothesised that the removal of singlet oxygen was responsible [5].

The paper covers the investigation into the phenomena beginning with the physics of the mechanism, the modelling of the positive corona process and the experiments to ascertain if there is any influence of singlet oxygen on the repetitive nature of positive corona.

2. CORONA IN AIR

The fundamentals of the gas discharge are presented in this section where the basics of deriving the Townsend and transport coefficients is key to understanding the following sections.

2.1 Collisional Cross-Sections

Molecules in a gas are in constant random motion and are constantly colliding with other molecules leading to a distribution of velocity or energy given by the Maxwell-Boltzmann distribution [6]:

$$f(v) = \left(\frac{m}{2\pi k_B T} \right)^{\frac{3}{2}} \exp\left(-\frac{mv_i^2}{2k_B T} \right) \quad (2)$$

Where:

- m = Mass of the particle [g]
- k_B = Boltzmann's constant
- T = Temperature [K]
- v_i = Velocity of particle [m.s⁻¹]

Applying an external influence such as change in temperature or an electric field (Lorentz force) would alter this distribution.

All of the collisional reactions (elastic and inelastic) are based on a probability phenomenon related to the energy (or velocity) of an electron and a collisional cross-section, σ , for each type of reaction [6].

The collisional cross-sections for nitrogen and oxygen are illustrated in Figure 1 and Figure 2. The cross-sections are based on the data collated by Itikawa [7–10]. The figure illustrates only the momentum, electronic excitation and ionisation cross sections. The data from the LXcat database, which is used for Bolsig+, is similar [11, 12].

It is evident that for an electron with any given energy that there are a number of reactions that could take place where the most likely is the momentum collision for the whole range of energies. As the electron energy increases the ionisation cross-section tends towards the momentum cross-section. There are multiple excited states of nitrogen, which act as energy sinks and is the reason it is often considered a good insulator, as these excited states retard the growth of a streamer. There are fewer excited states for oxygen when compared with nitrogen, there is however the additional attachment cross-section. It is evident that attachment is in a lower energy region of the graph when compared to the ionisation. Importantly singlet oxygen, $a^1\Delta_g$, has a cross-section that is spread over a wide range of energies.

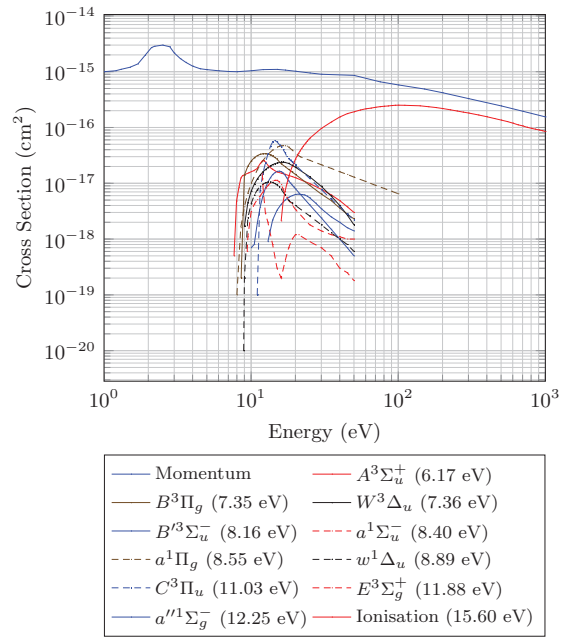


Figure 1: Collisional cross sections of nitrogen

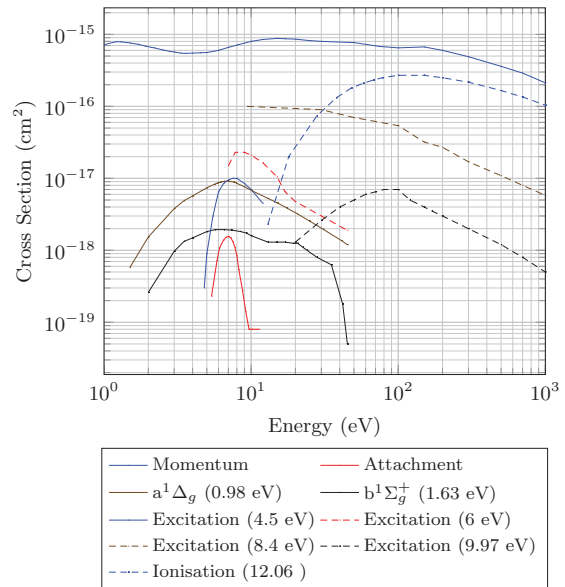


Figure 2: Collisional cross sections of oxygen

2.2 Townsend and Transport Coefficients

The Townsend and transport coefficients (mobility and diffusion) are derived from the cross-sections through the Boltzmann equation solver, Bolsig+ [13].

The Townsend coefficients and mean energy for an applied electric field are illustrated in Figure 3. The coefficients match well with published data [14]. It is seen that singlet oxygen has a relatively high Townsend coefficient indicating that singlet oxygen will be produced for wide range of applied electric fields. For a phenomena such

as corona where there is a non-linear electric field this indicates the singlet oxygen will be produced over the entire region.

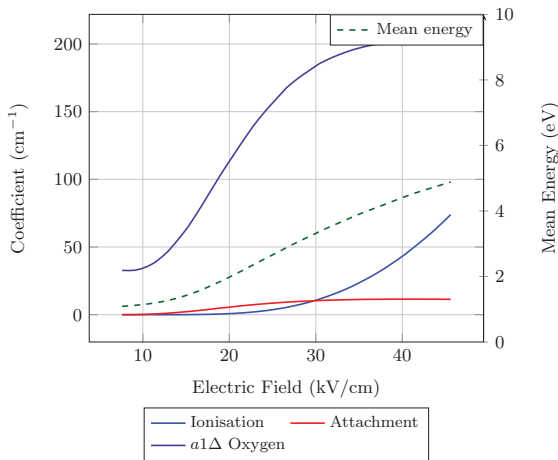


Figure 3: Townsend coefficients and mean electron energy for an applied electric field

2.3 Positive Corona

Positive corona is initiated by electrons that are freed due to natural processes in the air. The electron avalanche develops towards the electrode in an increasing electric field. The highest ionisation activity occurs near the conductor surface where the electric field is the highest [1, 2]. Clouds of space charge are formed which consist of mostly positive ions near the conductor and relatively small amounts negative ions away from the conductor as electrons are neutralised closer to the conductor. These space charge clouds modify the electric field and the discharge development leading to the modes of corona including Burst Corona, Onset Streamer, Positive Corona and Breakdown Streamer [1, 2].

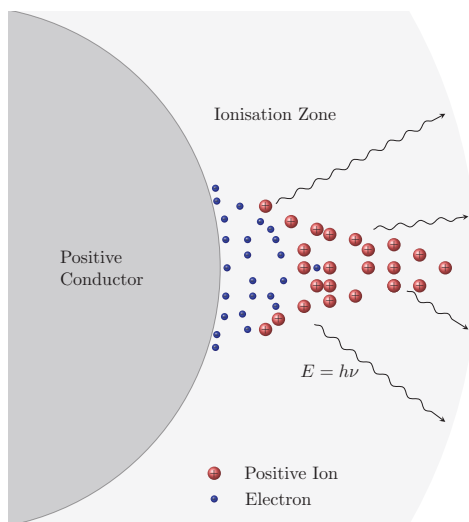


Figure 4: Positive corona

Burst corona occurs at the onset of positive corona where electrons lose their energy due to ionisation activities before they get absorbed by the conductor. The discharge directs radially outwards from the electrode. Positive ion space charge cloud is formed around the conductor which suppresses the discharge. The spread of electrons then moves to another part of the conductor. As the ionisation spreads around the conductor and is suppressed by the space charge cloud a positive corona current pulse is produced [1, 2].

Onset streamers result from radial development of the discharge. A large amount of positive ion space charge is left behind by electron avalanches and this space charge cloud enhances the electric field away from conductor, causing successive avalanches. The positive ion space charge cloud created from the avalanches reduces the electric field near the conductor surface and suppresses the streamer. When the space charge cloud is cleared, the original field is restored and the cycle repeats itself. The onset streamers have a pulse amplitude from a few milliamps to a few hundred milliamps, and the repetition rate increases with the voltage up to a critical point where it is then suppressed by the negative charge and the mode changes to glow. Positive onset streamers are the main source of radio interference and audio noise on transmission lines [1, 2]. The typical measured positive onset streamer pulse is illustrated in Figure 5.

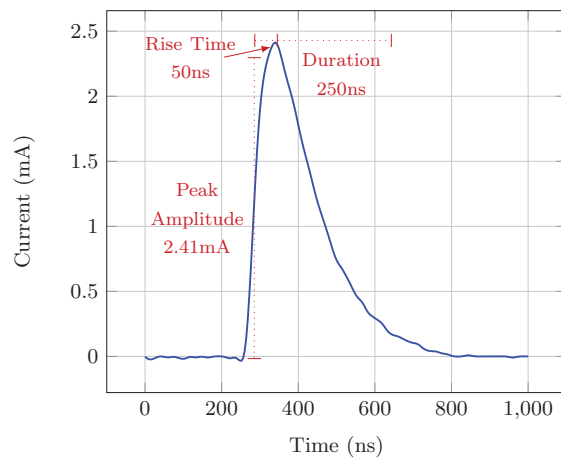


Figure 5: Positive onset streamer

Positive glow corona does not have a pulsating nature and occurs under a particular condition of production and removal of positive ions, where the field distribution allows for the rapid removal of positive ions while not allowing for the development of discharges and streamers. Glow corona manifests itself as a thin luminous layer over the conductor surface, where the discharge current is a direct current with a small superimposed pulsating current with a high repetition rate [1, 2].

Positive breakdown streamers are similar to onset streamers but extend further into the gap and lead to breakdown of the gap. The streamer current and repetition

rate are higher than onset streamers [1, 2].

3. MODELLING

The fluid model of a gas discharge is considered the most appropriate and successfully applied method to model the gas discharge.

Morrow et al proposed the use of the flux corrected transport algorithm (initially described by Boris and Book) as a numerical solution to the flow of charged particles in a gaseous system [15–19]. Morrow and Lowke applied the algorithm to the modelling of a streamer [15].

Shim et al further built on the FDM FCT methods for a two dimensional analysis of needle plane corona [20]. The finite difference schemes used in FCT however limit the shape of the grid, limit the type of complex geometries expected in discharges and can be computationally expensive. Georghiou et al proposed an improved finite element FCT method [21] and continued to implement it for various cases including the modelling of the gas discharge in two dimensions and investigating the role of photoionisation [22, 23]. Sattari et al have developed finite element methods to investigate Trichel pulses [24]. Deng et al have modelled the Trichel pulse under air flow conditions in two dimensions and successfully illustrated the influence the air flow on the space charge by showing that there was a decrease in repetition rate of Trichel pulses for 18 m.s^{-1} illustrate the effect of shifting the space charge [25]. The commercial package COMSOL Multiphysics[®] has become more popular in solving the drift diffusion equations and has been applied to gas discharges. Kim et al have investigated the breakdown voltage in air using COMSOL Multiphysics[®] [26]. Tran et al have investigated negative discharges in air with and without a dielectric barrier. The use of the fluid equations through COMSOL Multiphysics[®] in investigating surface charges on a dielectric barrier found good correlation with experiments [27]. Recently Zhuang and Zeng have developed a local discontinuous Galerkin method that combines the advantages of finite volume and finite element stating that it is a compact, local conservative and high order accurate method [28].

The FCT methods extend further into other research areas. Liu and Pasko, for example, have used similar algorithms to model positive and negative streamers that originate from quasi-static electric fields developed during lightning activity [29].

Whilst the authors have concentrated on negative corona and Trichel pulse, apart from the work done on positive glow by Morrow [15, 30], positive corona a modest presence in literature, possibly due to the unknown mechanisms that lead to initiation and possibly due to the space charge and electric field calculations for the discharge model.

The key to understanding the influence of singlet oxygen is to illustrate and understand the physical phenomena in

positive corona using the information from the solution of the Boltzmann equation and as such the 1.5D FDM model is considered sufficient.

3.1 Drift-Diffusion Model

The gas discharge is modelled using the drift-diffusion equations, where there are four species electrons, positive ions, negative ions and singlet oxygen. It is possible to extend this to any of the excited species but not necessary for the work here. The continuity equations written for the species in one dimension are given by [15–17, 19]:

$$\frac{\partial N_e}{\partial t} = S + N_e \alpha |\vec{v}_e| - N_e \eta |\vec{v}_e| - N_e N_p \beta - \frac{\partial(N_e \vec{v}_e)}{\partial z} + \frac{\partial}{\partial z} \left(D_e \frac{\partial^2 N_e}{\partial z^2} \right) \quad (3)$$

$$\frac{\partial N_p}{\partial t} = S + N_e \alpha |\vec{v}_e| - N_e N_p \beta - N_n N_p \beta - \frac{\partial(N_p \vec{v}_p)}{\partial z} + \frac{\partial}{\partial z} \left(D_p \frac{\partial^2 N_p}{\partial z^2} \right) \quad (4)$$

$$\frac{\partial N_n}{\partial t} = N_e \eta |\vec{v}_e| - N_n N_p \beta - N_n N_o k_d - \frac{\partial(N_n \vec{v}_n)}{\partial z} + \frac{\partial}{\partial z} \left(D_n \frac{\partial^2 N_n}{\partial z^2} \right) \quad (5)$$

$$\frac{\partial N_o}{\partial t} = N_e \Psi |\vec{v}_e| - N_n N_o k_d - N_o N_{O_2} k_q \quad (6)$$

Where:

- N_x = Number densities of electrons, positive ions, negative ions and singlet oxygen [cm^{-3}]
- N_{O_2} = Number density of oxygen [cm^{-3}]
- \vec{v}_x = Velocities of electrons, negative ions and positive ions [cm.s^{-1}]
- α = Ionisation coefficient [cm^{-1}]
- η = Attachment coefficient [cm^{-1}]
- Ψ = Singlet oxygen coefficient [cm^{-1}]
- S = Photoionisation term [$\text{cm}^{-3}.\text{s}^{-1}$]
- β = Recombination coefficient [$\text{cm}^3.\text{s}^{-1}$]
- D_x = Diffusion coefficient [$\text{cm}^2.\text{s}^{-1}$]
- k_d = Detachment rate coefficient [$\text{cm}^3.\text{s}^{-1}$]
- k_q = Quenching rate coefficient [$\text{cm}^3.\text{s}^{-1}$]

3.2 Photoionisation

A model of photoionisation was developed by Penny and Hummert, where they related the number of photo-electrons produced to the number of ionisation events [31]. They showed that the photoionisation events

are dependent on the pressure and distance from the discharge with a function given by [31].

$$\phi = \frac{N_p}{N_D} \theta PD \quad (7)$$

Where:

- N_D = Number of ion pairs produced per second
- N_p = Number of photon pairs produced per second
- PD = Pressure distance relationship [cm torr]
- θ = Angle subtended by volume

The physical model for photoionisation was developed by Zheleznyak et al [32] partially based on the data, where the model was based on the assumption that excited nitrogen atoms will emit in the region of 98 - 102.5 nm which is absorbed by oxygen with an ionisation threshold of 102.4 nm and this leads to photoionisation. The rate of photoionisation is dependent on the absorption of the emission and as such the partial pressure of oxygen [23, 32, 33]. Kulikovsky implemented a photoionisation model based on the the Zheleznyak model, where the number of electron-ion pairs produced per second in incremental volume dV_1 due to ionisation events in volume dV_2 is given by [33]:

$$S(dV_1, dV_2) \simeq \frac{I(dV_2)f(r)}{4\pi r^2} dV_2 \quad (8)$$

$$I(dV_2) = \xi \frac{P_q}{P + P_q} \alpha N_e \frac{dx}{dt} \quad (9)$$

$$f(r) = \frac{\exp(-\chi_{min} P_{O_2} r) - \exp(-\chi_{max} P_{O_2} r)}{r \log(\chi_{max}/\chi_{min})} \quad (10)$$

Where:

- r = Distance between volumes dV_1 and dV_2
- P = Pressure [760 torr]
- P_q = Quenching pressure [30 torr]
- P_{O_2} = Partial pressure of oxygen [22%P]
- $\chi_{max,min}$ = Absorption coefficients of O_2 [$\text{cm}^{-1} \cdot \text{torr}^{-1}$]

Pancheshnyi et al investigated the role of background ionisation and indicated that this background ionisation can be neglected when the photoionisation is included [34].

3.3 Electric Field

The electric field is solved through Poisson's equation, which describes the potential at a point [35]:

$$\nabla^2 \phi = -\frac{q_e}{\epsilon_0} (N_p + N_n + N_e) \quad (11)$$

Poisson's equation is solved with number densities set to 0 to obtain the Laplacian electric field E_L .

Davies stated that the using a uniform or cylindrical form of Poisson's equation overestimates the influence of the space charge on the electric field, as the discharge is only limited to a channel. A solution using disc's of space charge is that takes account of the radius of the channel r , is proposed where the Poissonian axial field at point along the axis is given by [19, 36, 37]:

$$E(x) = \frac{1}{2\epsilon_0} \int_{-x}^0 \rho(x+x') \left[-1 - \frac{x'}{\sqrt{x'^2 + r^2}} \right] dx' + \int_0^{d-x} \rho(x+x') \left[1 - \frac{x'}{\sqrt{x'^2 + r^2}} \right] dx' \quad (12)$$

The total field is then the sum of the Laplacian and Poissonian electric fields:

$$E = E_L + E_P \quad (13)$$

3.4 Circuit Current

Sato applied this concept to the movement of space charge in gas discharges and Morrow subsequently completed it to the form given by [38, 39]:

$$I(t) = \pi r^2 \frac{q_e}{V_A} \int_0^d (N_p v_p - N_n v_n - N_e v_e + \frac{\partial^2 D N_e}{\partial^2 x}) E_L dx \quad (14)$$

This form is however incomplete when relating it to the circuit as this current will affect the voltage applied to the test device [40]. The voltage applied to the test device is given by:

$$V_A = I(t)R - \frac{1}{C} \int I(t) dt \quad (15)$$

3.5 Results

The parameters used in the model are listed in Table 1.

An initial plasma number density is applied to the system, which gives a peak electron and positive ion density of 0.9995 cm^{-3} at 0.02 cm.

$$N_i = \exp(-(x+dx)^2) \quad (16)$$

The circuit current is illustrated in Figure 6 and it is followed by the pre-current pulse development of the electric field in Figure 7 and space charge in Figure 8 as well as the post current pulse development of the electric field in Figure 9 and space charge in Figure 10. The *Laplacian Field* refers to the electric field with no space charge and the *Space Charge Field* refers to the electric field determined only by the space charge. The *Total Field* is the sum of the two.

Table 1: Input parameters for positive corona model

Parameter/coefficient	Symbol	Value
Pressure	P	760 torr
Temperature	T	20 °C
Anode radius	r	0.02 cm
Electrode spacing	d	2.5 cm
Grid size	N_g	800
Grid spacing	dx	0.03 cm
Time step	dt	1×10^{-12}
Secondary ionisation	γ	0.01
Recombination	β	2×10^{-7}
Detachment	k_d	2×10^{-10}
Quenching	k_q	2×10^{-18}
Mobility of positive ion	μ_p	$2.34 \text{ cm}^2/\text{V/s}$
Mobility of negative ion	μ_n	$2.7 \text{ cm}^2/\text{V/s}$
Diffusion of positive ion	D_p	$5 \times 10^{-2} \text{ cm}^2/\text{s}$
Diffusion of negative ion	D_n	$5 \times 10^{-2} \text{ cm}^2/\text{s}$
Applied voltage	V_a	9 kV

It is clear that the in the process the role played by the positive ions far greater than the negative ions. The positive ions are generated rapidly at the electrode reaching a peak density of $2.4 \times 10^{13} \text{ cm}^{-3}$ after 30 ns, with the fast moving electrons at less than half this density after 50 ns. It is clear from Figure 7 that this distorts the field considerably causing a complete collapse near the electrode and a peak away from the electrode. This peak causes the streamer to propagate into the gap and the collapse prevents activity in the region close to the electrode. There will be no more ionisation activity until this space charge clears.

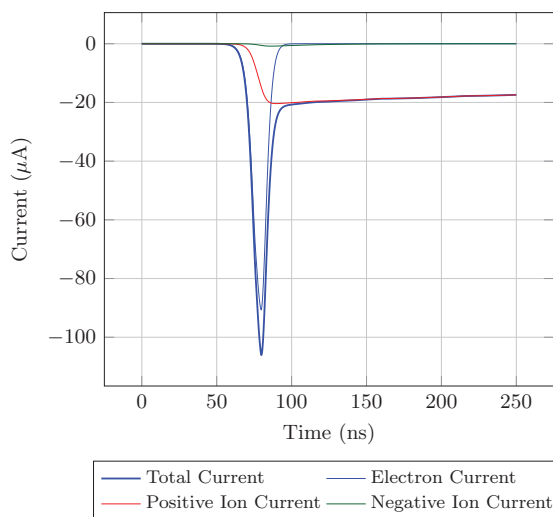


Figure 6: Circuit current for 250 μs

Following the distortion of the field in the initial pulse, the field recovers slowly. The densities of the species decrease due to the activities that occur where the field has collapsed including recombination of positive ions and

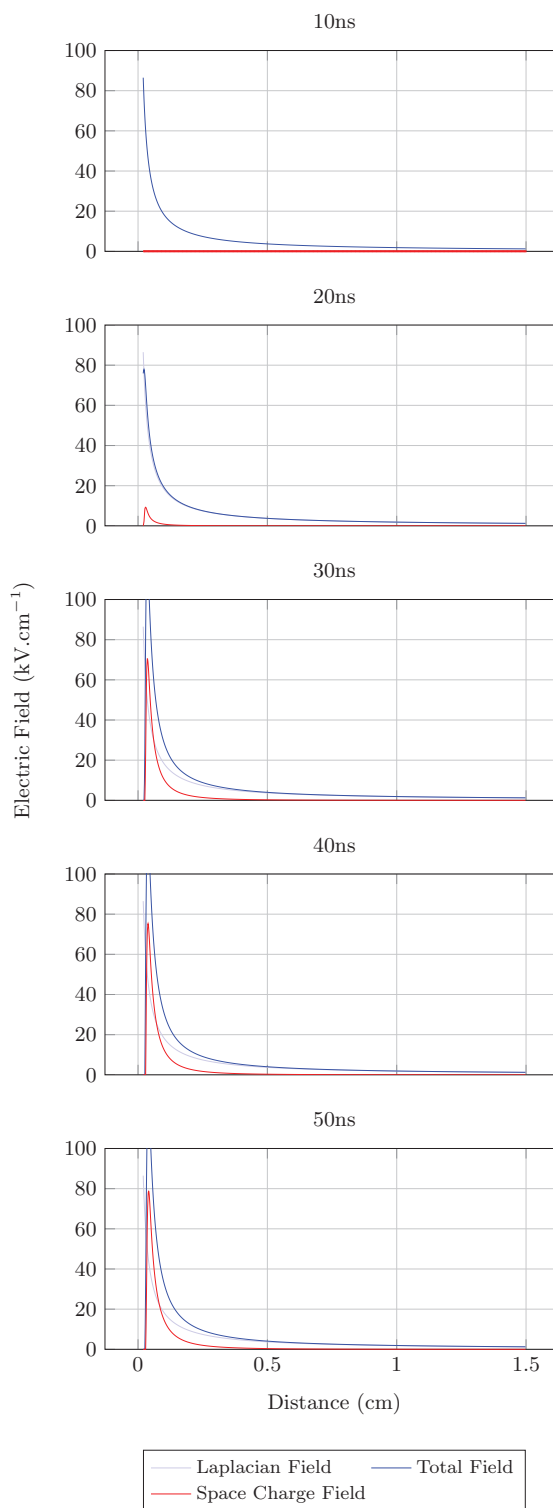


Figure 7: Electric field over 50 μs

electrons, recombination of negative ions, and detachment of electrons from the reaction of negative ions and singlet oxygen. There is no drift velocity as there is no electric field and as such the normal Townsend generation of species due to electron collision does not exist. While there is some value in the process, it is thought that the 1.5D

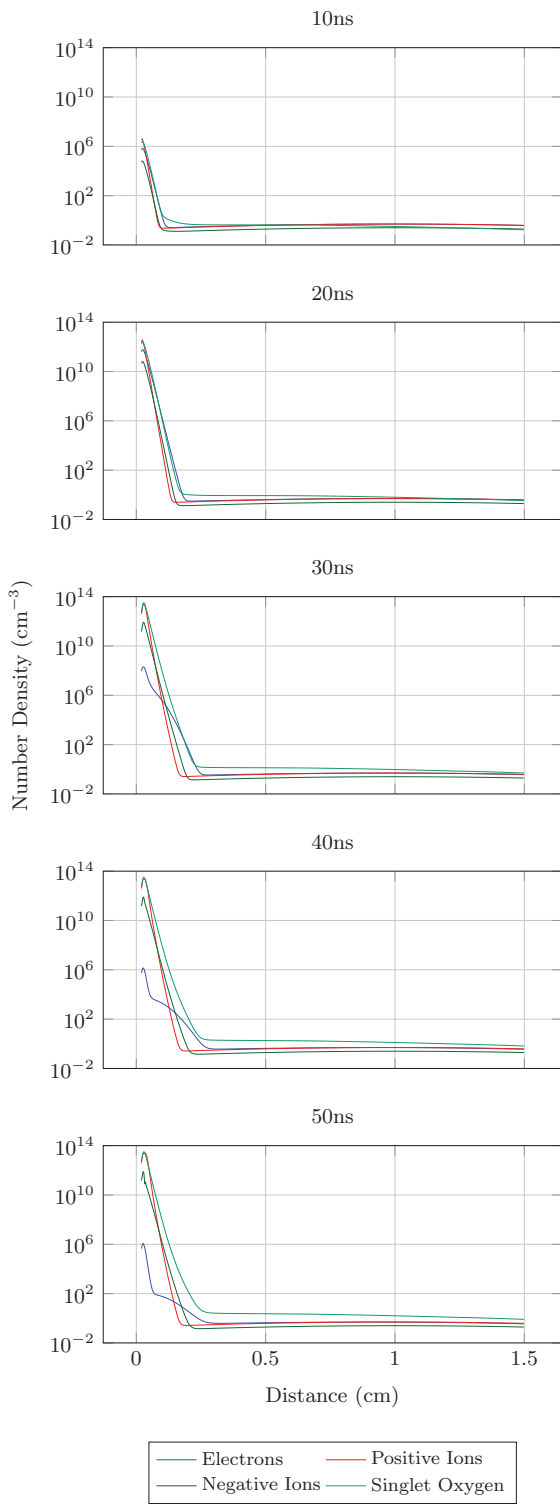


Figure 8: Number densities of species over 50 μ s

model is limited in this respect.

The oscillations seen at B occur only for the negative ions for the positive corona. These are thought to be numerical errors due to the recombination of positive and negative ions and to the reaction of negative ions and

singlet oxygen.

Singlet oxygen is generated within the region close to the cathode. After 4000 ns there is a peak singlet oxygen density of $8.5 \times 10^{12} \text{ cm}^3\text{s}^{-1}$ and a peak negative ion density of $3.92 \times 10^{10} \text{ cm}^3\text{s}^{-1}$. With a neutral density of $2.5 \times 10^{25} \text{ cm}^{-3}$ and a quenching rate of $2 \times 10^{-18} \text{ cm}^3\text{s}^{-1}$, the expected emission is 4.25×10^{11} photons per cm^3 per nanosecond. The emission is slightly higher than that of negative corona it is however localised around the anode.

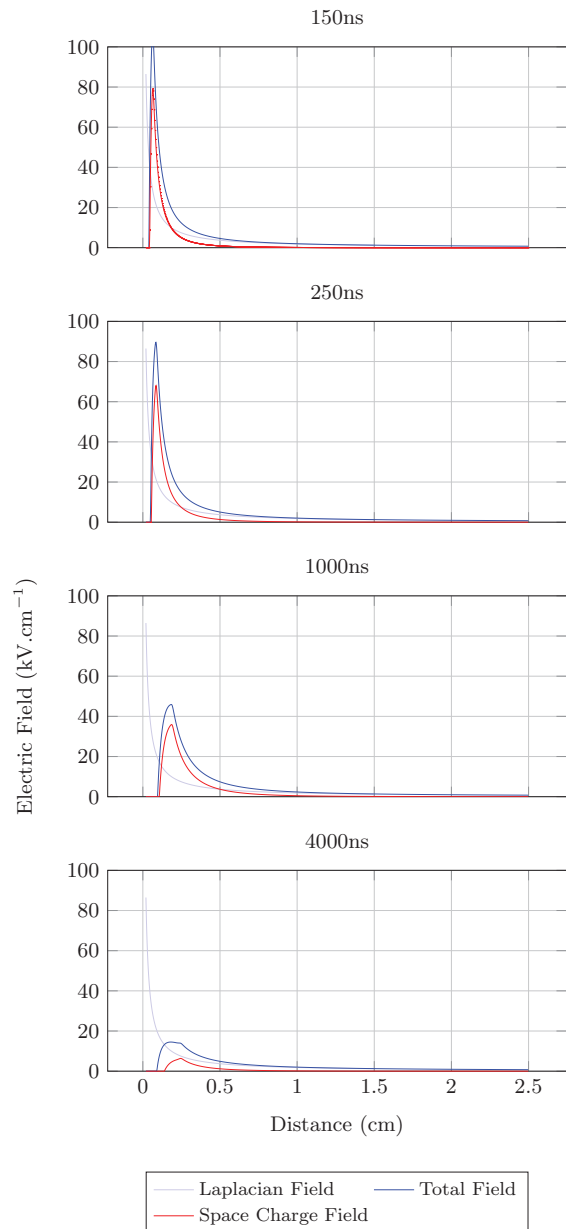


Figure 9: Electric field over the 4000 μ s

To illustrate the argument Figure 11 overlays the negative ion and singlet oxygen densities at 4000 ns by the detached electrons considering a detachment rate of $2 \times 10^{-7} \text{ cm}^3\text{s}^{-1}$ for the reaction between negative ions and

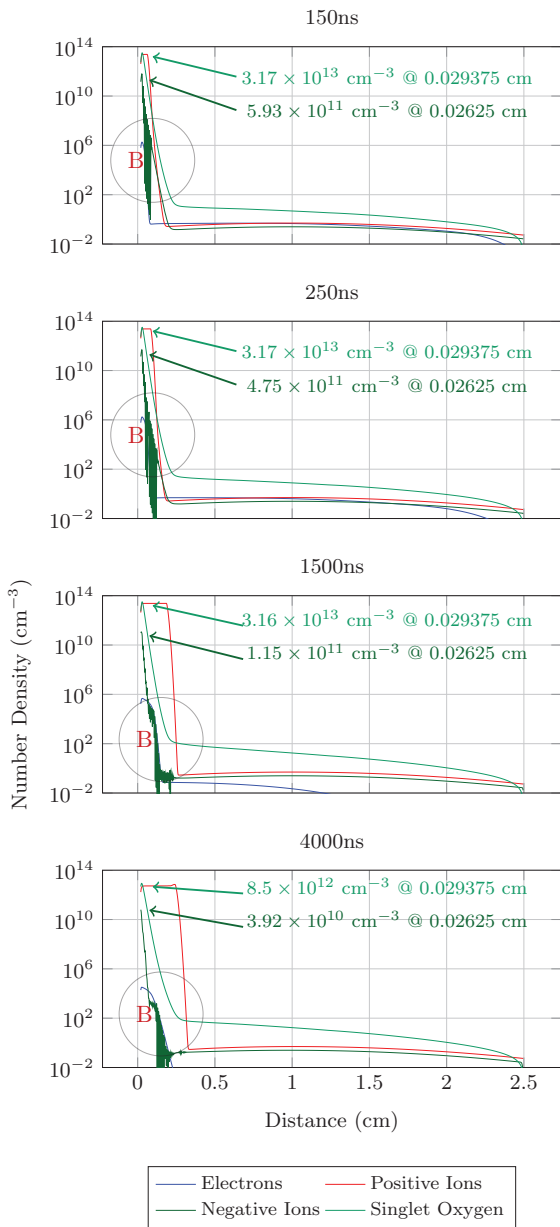


Figure 10: Number densities of species over 4000 μ s

singlet oxygen. This is slightly misleading as the negative ion and singlet oxygen densities are not constant over time and still decreasing, however, there is value in identifying that electrons are released. There is a peak rate of $2.55 \times 10^7 \text{ cm}^3.\text{ns}^{-1}$ at the anode and while this is a significant number, these electrons may be absorbed before impacting on the streamer. The rapid decline of detached electrons rate is clear in the plot and critical in extracting the influence of singlet oxygen. A higher density would be expected to initiate the streamer process, however the rate of $2.23 \text{ cm}^{-3}.\text{ns}^{-1}$ where $\alpha = \eta$ for the initial electric field illustrates that there may be a small correlation between the positive streamer and the singlet oxygen density should the field recover to its initial state. It is clear that the space charge is dominant and it takes a significant amount of time

to recover, in that time electrons may be formed by other means leaving those generated by singlet oxygen relatively insignificant. A number of experiments are undertaken in the next section to understand the significance.

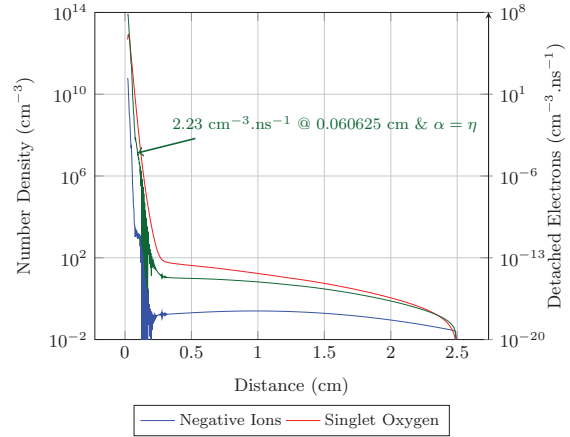


Figure 11: Negative ions and singlet oxygen densities overlaid by detached electrons

4. EXPERIMENTS

The experiment consisted of a point-plane configuration excited by a 50 kV DC source as shown in Figure 12. The point provided the necessary sharp electric field to produce positive onset streamers. The measurement system consisted of a voltage measured across a resistor below the second electrode. Gauss' law states that the measurement that the surface charge of the electrode will change according to the space charge inside of it [41].

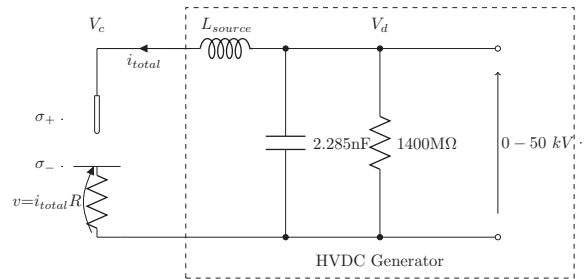


Figure 12: Experimental arrangement

4.1 Air Flow

The experiment was performed at the the high voltage laboratory at the University of the Witwatersrand which is located at an altitude of 1700 m. The experimental setup is illustrated in Figure 13 where a slow non-turbulent airflow of 5 m.s^{-1} was applied to the configuration. This is a continuation of the initial work in reference [5], where the hypothesis was formed.

The results in Figure 14 illustrate the approximate regions of burst, onset streamer and glow corona for the point plane

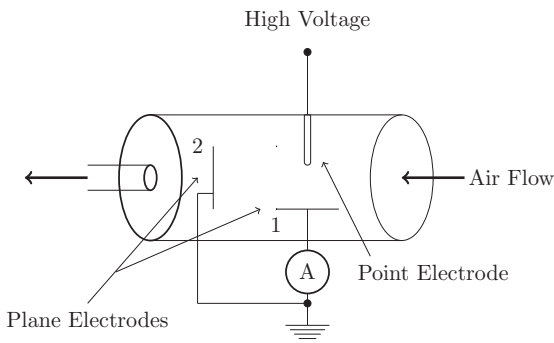


Figure 13: Experimental arrangement

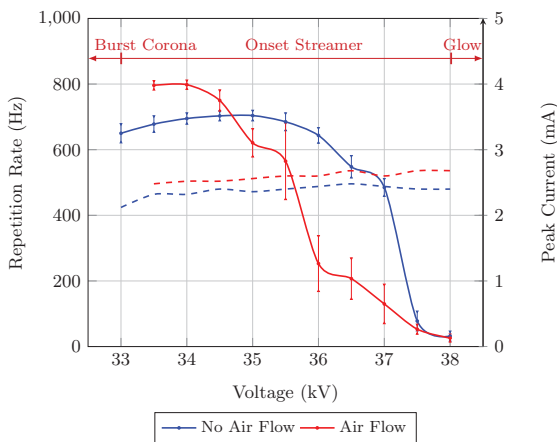


Figure 14: Measurement positive corona for airflow

experiment. It is evident that the air flow had an influence on the nature (and mode) of the corona, where initially the onset streamers increased in repetition rate and then sharply decreased in repetition rate. The average peak current was consistently higher for the air flow condition for all the applied voltages. The average peak current is dependent on the movement of the space charge and any small shift would cause the peak current to change slightly, which is evident in Figure 14.

The repetition rate of onset streamers are related to the collapse of the electric field at the conductor due to the positive space charge and the recovery due to the removal of the positive space charge [1], any influence on this space charge should theoretically result in an increase in the repetition rate as the field is restored faster. The results under air flow conditions were partially inconsistent with this theory.

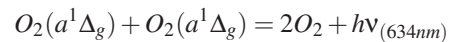
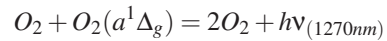
The fact that the average peak current has a relatively small deviation and the repetition rate has a large deviation lends credibility to the hypothesis that singlet oxygen may be a source of seed electrons and be related to the repetition rate of the onset streamers. The detachment of electrons from negative ions would be dependent on both the density of negative ions and singlet oxygen and the slow moving air removes the singlet oxygen from the system and does not

allow it to build up. Referring to the modelling of positive corona the densities of singlet oxygen and negative ions may not be large enough to react and produce sufficient seed electrons away from the anode to be the dominant process.

4.2 Infrared Detection

The purpose of the experiment was to measure a singlet oxygen emission and relate that to the repetition rate of positive onset streamers. Any relationship would indicate that it is a measurable and significant process.

The emissions of singlet oxygen due to the transition from singlet state to ground state or due to the dimol emission are given respectively by [42]:



Considering the Grum and Costa investigation into the spectral emission of corona [43]:

- 200-500 nm is the dominant region of emission with peaks at 337 nm and 358 nm due to transitions of nitrogen. This region of emissions have since been used as a basis for investigating corona on high voltage equipment [44].
- 400-600 nm where the peaks in the region of 400 nm are around 12.5% of the peaks in the UV region.
- 600-900 nm where the emissions are the lowest. There is activity around the 630-650 nm region, however there is no distinct peak in the region.

This as well as being the only emission in the region informed the decision to measure 1270 nm. The 1270 nm emission was investigated with an InGaAs pin photodiode as a detector [45]. Importantly the photosensitivity of the photodiode lies in the range of 900 nm to 1700 nm making it the optimal diode to detect the photo luminescence of singlet oxygen. As the only expected emission from corona in this region is from singlet oxygen, the use of a filter is deemed unnecessary. The use of the photodiode over a photomultiplier tube was due to the saturation of the latter in the presence of an electric field.

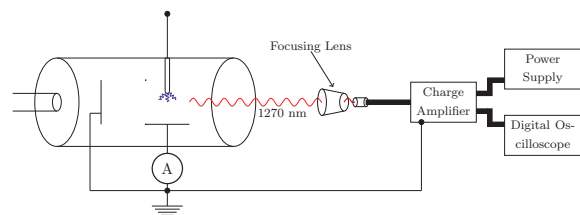


Figure 15: Experimental arrangement

The experiment was setup as illustrated in Figure 15 Figure 16 illustrates the optical emissions of the point plane gap in the visible region, where the extension of the onset streamers was approximately 1 cm from the anode surface. The infrared measurement system produced no detectable emissions from singlet oxygen, which could have been due to the weak emissions or due to detector sensitivity. The long lifetime of singlet oxygen does not assist with detection even if the densities are high. It has been noted that detection of singlet oxygen has been a difficult measurement to make in numerous fields including chemical and medical fields where more sensitive photomultiplier tubes have been used to detect it [46,47].

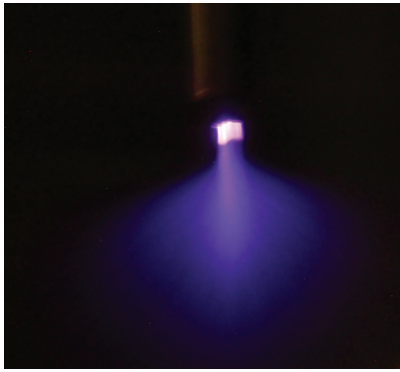


Figure 16: Onset streamer

4.3 Laser Excitation

The aim of the experiment was to determine the contribution of the singlet oxygen in the positive onset streamer by using a laser to excite the oxygen and observing the changes in waveform and repetition rate of the positive onset streamers. The advantage of this excitation due to the laser is that it isolates singlet oxygen and should have no effect on the space charge.

The Beer Lambert law relates the absorption capabilities of the material to the light and is given by [48]:

$$I = I_0 \exp(-\sigma N x) \tag{17}$$

Where:

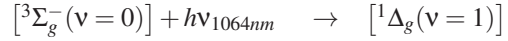
- I = Intensity
- I_0 = Initial intensity
- σ = Absorption cross-section
- N = Number density of the neutral
- x = Thickness of material

At 1.27 μm and 1.06 μm with peak cross sections of 2.52×10^{-26} and $0.717 \times 10^{-26} \text{ cm}^2 \cdot \text{molecule}^{-1}$ for a mixture of 21% O_2 and 79% N_2 at 20 °C and at an altitude of 1400 m; the intensity after 1 cm is $0.59I_0$ and $0.86I_0$ for 1.27 μm and 1.06 μm respectively [49].

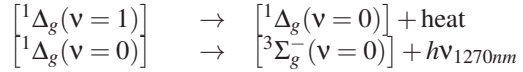
Jockusch et al have shown that oxygen is directly excitable through the use of an Nd:YAG laser with a wavelength of

1064 nm where the expected processes related to singlet oxygen include [46]:

The excitation process is [46]:



The emission processes are [46]:



The experiments were performed at the National Laser Centre at the CSIR at an altitude of 1400 m with a setup as illustrated in Figure 17. The laser was aimed approximately 1 cm below the electrode and each laser pulse had a 10 Hz frequency, a width of 10-20 ns, a beam diameter of 1cm (unfocused) and an energy of 118 mJ or 800 mJ.

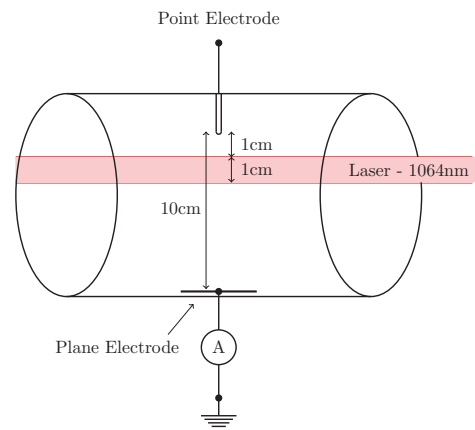


Figure 17: Experimental arrangement

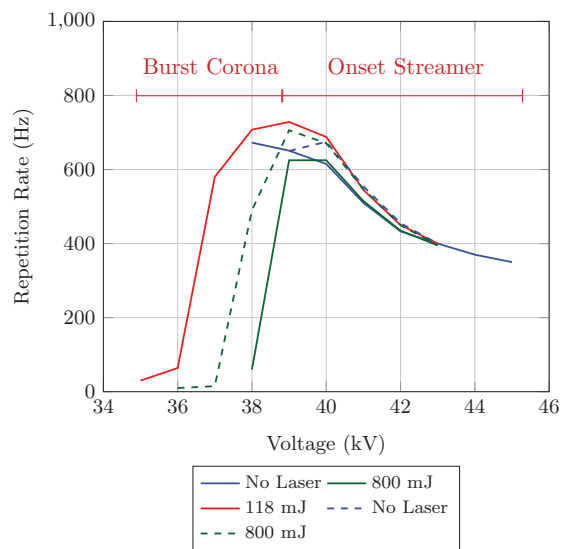


Figure 18: Measurement of positive corona for laser excitation

The repetition rate for positive onset streamers under normal conditions and for when the laser was fired in at

118 mJ and 800 mJ are illustrated in Figure ???. There are some differences at lower applied voltages, but tend to converge from 40 kV. Below 40 kV it was difficult to define the corona as onset streamers as it was inconsistent and it has been defined as burst corona. It is not evident that any singlet oxygen produced had an influence on the repetition rate of corona. The modelling illustrated that the singlet oxygen and negative ions produce high densities close to the anode, but are not produced further away where the reaction between negative ions and singlet oxygen does occur but is significantly less (Figure 11). It is felt by the author that the lack of negative ions in the region as shown by the modelling is critical, it is also evident that in the region where there are high densities of both negative ions and singlet oxygen, the ionisation, attachment and photoionisation mechanisms would be dominant.

5. CONCLUSION

The theory behind corona in air indicates that there are multiple excited states of its constituents. These excited states do play a role in the process, particularly where the energy of photons emitted from the excited molecules is high. The role of singlet oxygen was less well understood due to its low energy level and its secondary role of contributing to the production of seed electrons.

The modelling indicated that the influence of space charge on the collapse of the field for positive corona is the critical component of the pulse formation and duration. The model indicated that there is a presence of singlet oxygen, however the role it plays may be insignificant to that of the space charge.

The experiments investigated the role of singlet oxygen and illustrated that it is not a contributing factor to the positive onset streamers. This is inferred from the fact that

- The airflow influenced the removal of space charge and altered the repetition rate of positive onset streamers. The mode is pushed towards that of positive glow.
- The emission from singlet oxygen at 1270 nm was not detectable, both due to the low emission from singlet oxygen and sensitivity of the photodiode.
- The repetition rate does not change when oxygen is directly excited in the system through the use of a laser.

It is concluded that singlet oxygen plays no distinguishable role in the repetition rate of positive onset streamers as the production of seed electrons is minimal.

6. ACKNOWLEDGEMENTS

The authors would like to thank Eskom for the support of the High Voltage Engineering Research Group through the TESP programme. They would also like to thank

CBI-electric for support, the department of Trade and Industry (DTI) for THRIP funding as well as to the National Research Foundation (NRF) for direct funding.

The authors would like to thank Roel Stolper from the CSIR for the loan of lenses to aid in the detection experiments and Bathusile Masina and Thomas du Plooy from the CSIR National Laser Centre for allowing the use of the Nd:YAG laser for the experiments.

REFERENCES

- [1] P. Sarma Maruvada, *Corona Performance of High Voltage Transmission Lines*. Taylor and Francis Group, 2000.
- [2] T. Giao and J. Jordan, "Modes of corona discharges in air," *IEEE Transactions on Power Apparatus and Systems*, vol. 87, no. 5, 1968.
- [3] J. Lowke, "Theory of electrical breakdown in air - the role of metastable oxygen molecules," *Journal of Physics D: Applied Physics*, vol. 25, 1992.
- [4] J. Lowke and R. Morrow, "Theory of electric corona including the role of plasma chemistry," *Pure and Applied Chemistry*, vol. 66, no. 6, 1994.
- [5] A. Swanson, M. Grant, I. Hofsjager, and I. Jandrell, "HVDC corona - experimental setup and measurements," *International Symposium on High Voltage Engineering, Seoul, South Korea*, 2013.
- [6] E. Kuffel, W. Zaengl, and J. Kuffel, *High Voltage Engineering: Fundamentals*, 2nd ed. Newnes, 2000.
- [7] Y. Itikawa, M. Hayashi, A. Ichimura, K. Onda, K. Sakimoto, and K. Takayanagi, "Cross sections for collisions of electrons and photons with nitrogen molecules," *Journal of Physical Chemistry*, vol. 15, no. 3, 1986.
- [8] Y. Itikawa, "Cross sections for electron collisions with nitrogen molecules," *Journal of Physical Chemistry*, vol. 35, no. 1, 2006.
- [9] Y. Itikawa, A. Ichimura, K. Onda, K. Sakimoto, and K. Takayanagi, "Cross sections for collisions of electrons and photons with oxygen molecules," *Journal of Physical Chemistry*, vol. 18, no. 1, 1989.
- [10] Y. Itikawa, "Cross sections for electron collisions with oxygen molecules," *Journal of Physical Chemistry*, vol. 38, no. 1, 2009.
- [11] A. Phelps and L. Pitchford, "Anisotropic scattering of electrons by N₂ and its effect on electron transport," *Phys. Rev. A*, vol. 31, no. 5, 1985.
- [12] Plasma Data Exchange Project, "Lxcat," <http://fr.lxcat.net/home/>, last accessed March 12, 2015.

- [13] G. Hagelaar and L. Pitchford, "Solving the boltzmann equation to obtain electron transport coefficients and rate coefficients for fluid models," *Plasma Sources Science and Technology*, vol. 14, 2005.
- [14] A. Swanson, M. Grant, and I. Jandrell, "HVDC corona - analysis of corona through modelling techniques," *International Symposium on High Voltage Engineering, Seoul, South Korea*, 2013.
- [15] R. Morrow and J. Lowke, "Streamer propagation in air," *Journal of Physics D: Applied Physics*, vol. 30, 1997.
- [16] R. Morrow, "Numerical solution of hyperbolic equations for electron drift in strongly non-uniform electric fields," *Journal of Computational Physics*, 1981.
- [17] R. Morrow and L. Crem, "Flux-corrected transport and diffusion on a non-uniform mesh," *Journal of Computational Physics*, 1985.
- [18] J. Boris and D. Book, "Flux-corrected transport. I. SHASTA, a fluid transport algorithm that works," *Journal of Computational Physics*, 1973.
- [19] R. Morrow, "Theory of negative corona in oxygen," *Phys. Rev. A*, 1985.
- [20] J. Shim, S. Choi, H. Hwang, H. Ha, K. Ko, and H. Kang, "2-d simulation on the corona discharge of negative needle-to-plane electrodes," *IEEE Transactions on Magnetics*, vol. 38, no. 2, 2002.
- [21] G. Georghiou, R. Morrow, and A. Metaxas, "An improved finite-element flux-corrected transport algorithm," *Journal of Computational Physics*, vol. 148, 1999.
- [22] —, "A two-dimensional, finite-element, flux-corrected transport algorithm for the solution of gas discharge problems," *Journal of Physics D: Applied Physics*, vol. 33, 2000.
- [23] A. Hallac, G. Georghiou, and A. Metaxas, "Secondary emission effects on streamer branching in transient non-uniform short-gap discharges," *Journal of Physics D: Applied Physics*, vol. 36, 2003.
- [24] P. Sattari, C. Gallo, S. Castle, and K. Adamaniak, "Trichel pulse characteristics—negative corona discharge in air," *Journal of Physics D: Applied Physics*, vol. 44, 2011.
- [25] F. Deng, L. Ye, and K. Song, "Numerical studies of trichel pulses in airflows," *Journal of Physics D: Applied Physics*, 2013.
- [26] N. Kim, S. Lee, G. Georghiou, D. Kim, and D. Kim, "Accurate prediction method of breakdown voltage in air at atmospheric pressure," *Journal of Electrical Engineering and Technology*, vol. 7, 2012.
- [27] T. Tran, I. Golosnoy, P. Lewin, and G. Georghiou, "Numerical modelling of negative discharges in air with experimental validation," *Journal of Physics D: Applied Physics*, vol. 44, 2011.
- [28] Zhuang and Zeng, "A local discontinuous galerkin method for 1.5-dimensional streamer discharge simulations," *Applied Mathematics and Computation*, vol. 219, 2013.
- [29] N. Liu and V. Pasko, "Effects of photoionization on propagation and branching of positive and negative streamers in sprites," *Journal of Geophysical Research*, vol. 109, 2004.
- [30] R. Morrow, "The theory of positive glow corona," *Journal of Physics D: Applied Physics*, vol. 30, 1997.
- [31] G. Penney and G. Hummert, "Photoionization measurements in air, oxygen and nitrogen," *Journal of Applied Physics*, vol. 41, no. 2, 1970.
- [32] M. Zheleznyak, B. Mnatskanian, and S. Sizykh, "Photoionization of nitrogen and oxygen mixtures by radiation from gas discharge," *High Temperature*, 1982.
- [33] A. Kulikovskiy, "The role of photoionization in positive streamer dynamics," *Journal of Physics D: Applied Physics*, vol. 33, 2000.
- [34] S. Pancheshnyi, S. Starikovskaia, and A. Y. Starikovskii, "Role of photoionization process in propagation of cathode-directed streamer," *Journal of Physics D: Applied Physics*, vol. 34s, 2001.
- [35] J. Kraus, *Electromagnetics*, 4th ed. McGraw-Hill, Inc, 1991.
- [36] A. Davies, C. Evans, and F. Llewellyn Jones, "Electrical breakdown of gases: The spatio-temporal growth of ionization in fields distorted by space charge," *Proceedings of the Royal Society of London - Series A: Mathematical and Physical Sciences*, vol. 281, no. 1385, 1964.
- [37] A. Davies, "Discharge simulation," *IEE Proceedings A*, vol. 133, no. 4, 1986.
- [38] N. Sato, "Discharge current induced by the motion of charged particles," *Journal of Physics D: Applied Physics*, vol. 13, 1980.
- [39] R. Morrow and N. Sato, "The discharge current induced by the motion of charged particles in time-dependent electric fields; Sato's equation extended," *Journal of Physics D: Applied Physics*, vol. 32, 1999.
- [40] J. Verboncoeur, M. Alves, V. Vahedi, and C. Birdsall, "Simultaneous potential and circuit solution for 1d bounded plasma particle simulation codes," *Journal of Computational Physics*, vol. 104, 1993.

- [41] C. Birdsall, "Particle-in-cell charged particle simulations, plus Monte Carlo collisions with neutral atoms, pic-mcc," *IEEE Transactions on Plasma Science*, vol. 19, no. 2, 1991.
- [42] D. Kearns, "Physical and chemical properties of singlet oxygen," *Chemical Reviews*, vol. 71, no. 4, 1971.
- [43] F. Grum and L. F. Costa, "Spectral emission of corona discharges," *Appl. Opt.*, vol. 15, no. 1, pp. 76–79, Jan 1976. [Online]. Available: <http://ao.osa.org/abstract.cfm?URI=ao-15-1-76>
- [44] W. Vosloo, R. Stolper, and P. Baker, "Daylight corona discharge observation and recording system," *International Symposium on High Voltage Engineering, Quebec, Canada, 1997*.
- [45] Hamamatsu, "InGaAs PIN Photodiodes - G8376 Series," <http://www.hamamatsu.com>, last accessed 2013.
- [46] S. Jockusch, N. Turro, E. Thompson, M. Gouterman, J. Callis, and G. Khalil, "Singlet molecular oxygen by direct excitation," *The Royal Society of Chemistry: Photochemical and Photobiological Sciences*, 2008.
- [47] M. Niedre, M. Patterson, and B. Wilson, "Direct near-infrared luminescence detection of singlet oxygen generated by photodynamic therapy in cells in vitro and tissue in vitro," *Photochemistry and Photobiology*, vol. 75, 2002.
- [48] R. Serway and R. Beichner, *Physics for Scientists and Engineers with Modern Physics*, 5th ed. Saunders College Publishing, 2000.
- [49] K. Smith and D. Newham, "Near-infrared absorption cross-sections and integrated absorption intensities of molecular oxygen (O_2 , $O_2 - O_2$ and $O_2 - N_2$)," *Journal of Geophysical Research*, vol. 105, no. D6, 2000.